1871
ИнБЮМ – IBSS

Морской биологический журнал
Marine Biological Journal
2026, vol. 11, no. 2, pp. 67–84
https://marine-biology.ru/mbj/article/view/524

UDC [581.526.325:57.017.7](265.51/.53)

PHYTOPLANKTON PHOTOSYNTHETIC PARAMETERS IN WATERS NEAR THE KAMCHATKA PENINSULA IN AUGUST–SEPTEMBER 2023

© 2026 **T. Efimova[1,2], T. Churilova[1,2], N. Moiseeva[1], E. Skorokhod[1,2], P. Salyuk[3], and A. Yatsuk[4]**

[1]A. O. Kovalevsky Institute of Biology of the Southern Seas of RAS, Sevastopol, Russian Federation
[2]Laboratory of Ecology and Evolutionary Biology of Hydrobionts, Institute of the World Ocean, Far Eastern Federal University, Vladivostok, Russian Federation
[3]V. I. Il'ichev Pacific Oceanological Institute FEB RAS, Vladivostok, Russian Federation
[4]Sirius University of Science and Technology, Sirius, Russian Federation
E-mail: *tatyana-iefimova@yandex.ru*

Received: 17.06.2025; revised: 17.06.2025;
accepted: 12.02.2026.

The climate change and increasing anthropogenic load affect the aquatic ecosystems. State and productivity of pelagic ecosystems are largely determined by photosynthetic capacity of phytoplankton. The aim of this work was to analyze the variability of phytoplankton photosynthetic parameters [quantum yield of photosynthesis (ϕ) which characterizes efficiency of absorbed light quanta utility in photosynthesis, its potential capacity (ϕ_{max}), and light-saturation coefficient (I_k)] depending on light conditions, which are determined by the ratio of thickness of the upper mixed layer (UML) to the depth of the euphotic zone (Z_{eu}). The study covered data obtained in the Pacific Ocean and the Sea of Okhotsk during the cruise 23/4 of the RV "Professor Multanovskiy" in August–September 2023. Parameters ϕ_{max} and I_k were calculated based on measurements of rapid light–response curves of variable fluorescence. As found out, variability in photosynthetic parameters was mainly determined by phytoplankton physiological acclimation to light. Importantly, acclimation to light, which differed between the UML and the deeper layer of the Z_{eu}, resulted in distinct light–response patterns of relative electron transport rate curves. The values of I_k were directly related to light intensity. Nonetheless, the values of ϕ_{max} were inversely related to light intensity, but to a larger extent than the values of I_k. As a result, ϕ, which depends on I_k and ϕ_{max}, dropped with increasing light intensity. A tight relationship between the values of ϕ and light intensity ($r = 0.97$) was revealed ($p < 0.0001$), and it was described by an exponential function. This analysis showed peculiarities of the light forcing variability in photosynthetic parameters. The revealed dependences of I_k, ϕ_{max}, and ϕ on light intensity can be used for express assessment of their values based on light; this is necessary for analysis of primary production involving spectral approach.

Keywords: chlorophyll fluorescence, photoacclimation, rapid light–response curve, quantum yield of photosynthesis, Pacific Ocean, Sea of Okhotsk

All life on Earth is supported by the process of primary production (hereinafter PP). PP is formed by the conversion of inorganic compounds (water and carbon dioxide) into organic ones (carbohydrates) during photosynthesis. In aquatic ecosystems, phytoplankton is the most important primary producer [Evolution of Primary Producers, 2011]. Since photosynthesis requires light quanta, phytoplankton inhabits the upper water layer, where there is enough light. Within the euphotic zone (hereinafter Z_{eu}), phytoplankton deals with various environmental conditions. Vertical water stratification divides

the water column into quasi-isolated layers and limits the water exchange between the upper mixed layer (hereinafter UML) and the layer between the UML bottom (Z_{UML}) and the Z_{eu}. As a result of stratification within the Z_{eu}, phytoplankton inhabits water layers (UML and layer below the UML) with different nutrient availability, temperature, and light, and this affects photosynthesis rate and PP. Precise assessment of PP is necessary to study patterns of primary synthesis of organic matter in the World Ocean, which is crucial in the context of global warming and increasing anthropogenic load. Spectral PP algorithms [Churilova et al., 2016; Morel et al., 1996; Smyth et al., 2005], which take into account the spectral features of light and the light absorption capacity of phytoplankton, provide a more correct PP assessment than other algorithms. The spectral PP model is based on phytoplankton photosynthetic parameters: light intensity saturating the photosynthesis rate and values of maximum quantum yield of photosynthesis (ϕ_{max}), which characterize efficiency of absorbed quanta utility in the organic matter synthesis.

Traditionally, photosynthesis-irradiance curves (P-I) are used for the quantitative characterization of the light-dependent photosynthetic activity of photoautotrophs [Platt, Jassby, 1976; Platt et al., 1980]. P-I curves are built by measuring photosynthesis rates under a range of light intensity levels and provide information on photosynthetic characteristics of phytoplankton. P-I curves supply data on physiologically meaningful parameters which can be estimated by mathematical models describing the general photosynthetic light–response pattern [Bannister, 1979; Platt et al., 1980]. Steady-state P-I relationships allow characterizing photoacclimation status of cells formed as a response to long-term light exposure conditions, by means of the maximum photosynthesis rate, the tangent of initial slope of P-I curve, and light intensity saturating the photosynthesis rate [MacIntyre et al., 2002; Platt et al., 1980].

The application of fluorometric methods allowed rapid assessment of *in vivo* photosynthesis by monitoring the activity of photosystem II (hereinafter PSII) [Schreiber et al., 1994] using rapid light–response curves (hereinafter RLCs) of relative electron transport rate (rETR). Although rETRs in PSII characterize status of cell photoacclimation to recent light history (short-term photoacclimation) [Schreiber et al., 1997], RLCs may also provide information on long-term photoacclimation status, as obtained by P-I curves [Cruz, Serôdio, 2008; Serôdio et al., 2006]. Consequently, RLCs are particularly useful for the study of the photosynthetic activity of phytoplankton in different water layers within the Z_{eu}. Specifically, based on RLC parameters, light intensity saturating the rETR (I_k) and ϕ_{max} can be estimated [Schreiber et al., 1997].

The light-saturation coefficient I_k is determined as light intensity at which photosynthesis reaches saturation and equals the maximum rETR ($rETR_{max}$) divided by tangent of initial slope of RLC (α) [Schreiber et al., 1994]. Maximum quantum yield of PSII (F_v/F_m) is transformed to quantum yield of photosynthesis ϕ_{max} based on electron requirement for carbon fixation (K_C) [Lawrenz et al., 2013]. According to the classical Z-scheme for photosynthetic electron transfer, it takes four electrons (e^-) to transport through photosynthetic electron transport chain to fix one CO_2 molecule [Falkowski, Raven, 2007]. Most studies use K_C of 5 mol e^- / mol C to convert ETRs to carbon fixation rates, assuming that four e^- transported through photosynthetic electron transport chain are required for O_2 molecule produced, and that photosynthetic quotient is 1–1.5 mol O_2 / mol CO_2 [Laws, 1991]. However, it was shown that the vast majority of K_C estimates in various regions were in a range within 1.2–54 mol e^- / mol C with a mean of (11 ± 7) mol e^- / mol C [Lawrenz et al., 2013]. Multivariate analysis of data for the Ariake Bay [Zhu et al., 2016], the East China Sea, the Tsushima Strait [Zhu et al., 2017], and the Arctic Ocean [Zhu et al., 2019] revealed a strong correlation between daily photosynthetically available radiation (hereinafter PAR) and K_C. This should be taken into account when calculating ϕ_{max}.

The aim of the study was to analyze the variability of photosynthetic parameters of phytoplankton measured by fluorimetry. This was necessary for assessment of primary production and the state of the pelagic ecosystem of shelf waters near the Kamchatka Peninsula in August–September 2023.

MATERIAL AND METHODS

Water sampling. Sampling was carried out during the cruise 23/4 of the RV "Professor Multanovskiy," 17 August – 11 September, 2023, in waters near the Kamchatka Peninsula (the Sea of Okhotsk and the Pacific Ocean) (Fig. 1).

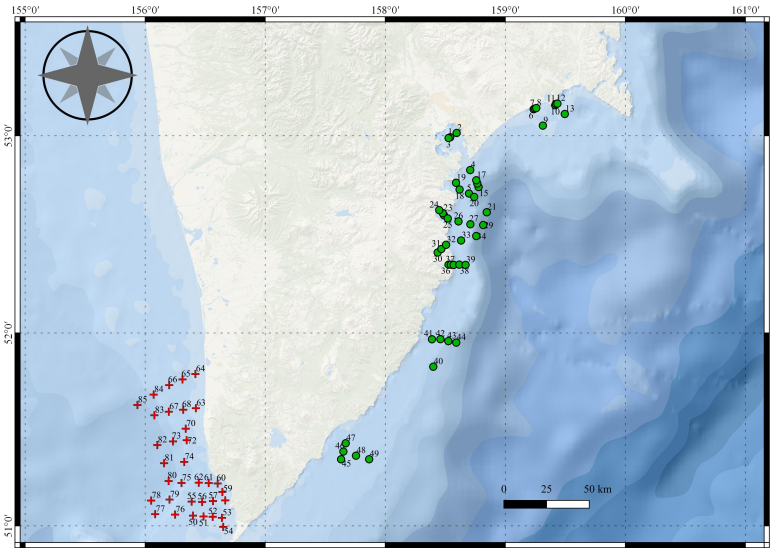

Fig. 1. Stations during the cruise 23/4 of the RV "Professor Multanovskiy," 17 August – 11 September, 2023, in the Pacific Ocean (●) and the Sea of Okhotsk (+)

Рис. 1. Станции рейса 23/4 НИС «Профессор Мультановский», 17 августа — 11 сентября 2023 г., в Тихом океане (●) и Охотском море (+)

Within one day, sampling was carried out over an area of no more than 30 km × 30 km. Water was sampled from several depths within the Z_{eu} in the daytime, 8:00–19:00. The Z_{eu} was determined as a depth where PAR was reduced to 1% of the PAR incident on the water surface (PAR_0). PAR was continuously measured with a LI-COR portable photosynthesis system with a temporal resolution of 1 s. Sampling depths were chosen based on vertical distribution of temperature, salinity, PAR, and chlorophyll *a* fluorescence. Sampling was carried out with Niskin bottles mounted on a frame equipped with SBE oceanographic complex (Sea-Bird Scientific) and CTD profiler. Chlorophyll *a* fluorescence was measured with submersible WETStar fluorometer W535-1246. Variable fluorescence of all samples collected at the station was measured for ~ 1 h after sampling.

Z_{UML} was assessed using the density difference criterion (0.2 kg·m^{-3}) from a near-surface value at a depth of 1 m [Brainerd, Gregg, 1995]. PAR in the UML (PAR_{UML}) was calculated according to [Babin, 2008]:

$$PAR_{UML} = PAR_0 \times \frac{1 - e^{K_d Z_{UML}}}{K_d Z_{UML}} .$$

Diffuse attenuation coefficient of light (K_d) was determined as follows [Babin et al., 1996]:

$$K_d = \frac{4.6}{z_{eu}} .$$

Values of PAR at different depths (PAR_Z) were calculated according to [Kirk, 2011]:

$$PAR_Z = PAR_0 \times e^{-K_d z} .$$

Water layer of the first optical depth equals $1 / K_d$ [Lee et al., 2007].

Fluorescence measurements. Variable fluorescence was determined with a chlorophyll *a* fluorescence kinetic measurement system Smart (Department of Biophysics, Faculty of Biology, Moscow State University, Russia) [Antal et al., 2019]. A blue LED with maximum emission at 445 nm generates either strong actinic light pulses (photon flux density, PFD, of 5,000 μmol·m^{-2}·s^{-1}) or short measuring pulses. *Prior* to the start of variable fluorescence measurements, water samples were dark-incubated for at least 30 min [Babin, 2008]. The fluorescence of samples was corrected by subtraction of fluorescence yield of colored dissolved organic matter (F_{CDOM}) to get phytoplankton fluorescence yield. To determine F_{CDOM}, samples were filtered through nucleopore filters (pore diameter of 0.2 μm) under low vacuum (< 25 kPa). Nucleopore filters were pre-washed with deionized water [IOCCG, 2019]. The water samples were pre-filtered through glass microfiber filters (GF/F).

Minimum fluorescence yield (F_0), maximum fluorescence yield (F_m), and F_v/F_m were determined for dark-adapted phytoplankton. F_v was calculated as $F_m - F_0$ [Schreiber et al., 1994]. RLCs of rETR *vs.* PFD were measured at 29 PFD levels (exposition of 20 s), from 0.0125 to 1,000 μmol·m^{-2}·s^{-1}.

RLCs were fitted using the model of [Platt et al., 1980]:

$$rETR = rETR_{max} \times \left[1 - \exp\left(-\frac{\alpha PAR}{rETR_{max}}\right)\right] \exp\left(-\frac{\beta PAR}{rETR_{max}}\right),$$

where β is tangent of slope of rETR-light curve on declining section.

RLC fits were very good, with $r > 0.95$ for a total of 214 light curves.

I_k was determined applying parameters of RLC [Cruz, Serôdio, 2008]:

$$I_k = \frac{rETR_{max}}{\alpha}.$$

The parameter ϕ_{max} was calculated as follows:

$$\phi_{max} = (F_v/F_m)/(2K_C),$$

where 2 is conversion factor of electron requirement for carbon fixation to quantum requirement for carbon fixation.

The values of K_C (mol e$^-$ / mol quanta) were derived from relationships between PAR (mol·m^{-2}·day^{-1}) and K_C [Zhu et al., 2017]:

$$K_C = 0.85PAR + 6.55.$$

The values of φ were calculated according to [Marra et al., 2000]:

$$\phi = \phi_{max} \times tanh(I_k/PAR).$$

Statistical analyses. Kolmogorov–Smirnov and Shapiro–Wilk tests were applied to examine the data for normality. The mean ± standard deviation (*SD*) allowed describing the variability within the data group. Statistical analysis involved Grapher v17 and Statistica 12 software. The map of stations was plotted with QGIS desktop 3.8.0 software. The figures were plotted applying Grapher v17.

RESULTS

Hydrophysical properties. In August–September 2023, the study area was heterogeneous in terms of water transparency. The Z_{eu} values varied by about 5 times: from 8 m in coastal waters to 47 m in shelf waters; the mean was (21 ± 6) m (Table 1). Lower Z_{eu} values, averaging (10 ± 2) m, were recorded in the Pacific Ocean: in the Avacha Bay, the Zhirovaya Bay, the Russkaya Bay, and near the Khalaktyrsky Beach on the eastern coast of the Kamchatka Peninsula. The first optical depth varied from 1.3 to 7.6 m.

Table 1. Hydrophysical characteristics in waters near the Kamchatka Peninsula in August–September 2023: photosynthetically available radiation incident on the water surface (PAR_0); photosynthetically available radiation in the upper mixed layer (PAR_{UML}); depth of the upper mixed layer (Z_{UML}); depth of the euphotic zone (Z_{eu}); salinity at the surface (S); water temperature at the surface (T); and maximum density gradient ($\Delta\sigma_{max}$)

Таблица 1. Гидрофизические характеристики шельфовых вод Камчатского полуострова в августе — сентябре 2023 г.: фотосинтетически активная радиация, падающая на поверхность моря (PAR_0); фотосинтетически активная радиация в верхнем квазиоднородном слое (PAR_{UML}); глубина верхнего квазиоднородного слоя (Z_{UML}); глубина зоны фотосинтеза (Z_{eu}); солёность на поверхности (S); температура воды на поверхности (T); максимальный градиент плотности ($\Delta\sigma_{max}$)

	PAR_0, mol·m^{-2}·day^{-1}	PAR_{UML}, mol·m^{-2}·day^{-1}	Z_{UML}, m	Z_{eu}, m	S, psu	T, °C	$\Delta\sigma_{max}$, kg·m^{-3}
Pacific Ocean							
Mean	23.0	14	3.9	20	30	+14	0.62
SD	9.7	6.7	2.4	6.4	1.5	1.5	0.40
Min	6.2	3	2	8	23	+9.9	0.20
Max	38.0	27	11	35	32	+16	2.5
Sea of Okhotsk							
Mean	19.0	7.2	11	27	32.3	+11	0.22
SD	11.0	5.8	6.3	9.8	0.40	1.6	0.16
Min	4.7	0.77	2	14	30.5	+7.5	0.019
Max	33.0	22	24	47	32.6	+13	0.74

Sea surface temperature in waters near the Kamchatka Peninsula varied in the range of +7.5…+16.0 °C. The values decreased in the direction from the Pacific Ocean [+9.9…+16.0 °C; the mean of (+14.0 ± 1.5) °C] to the Sea of Okhotsk [+7.5…+13.0 °C; the mean of (+11.0 ± 1.6) °C] (see Table 1).

Sea surface salinity in the Sea of Okhotsk fluctuated in a narrow range: from 30.5 to 32.6 psu. In the Pacific Ocean, sea surface salinity dropped from 32.0 psu near the southeastern Kamchatka Peninsula to 23.0 psu in the Avacha Bay. The high desalination in the Avacha Bay is associated with intensive coastal runoff. In the Pacific Ocean, the maximum density gradient [the mean of (0.62 ± 0.40) kg·m^{-3}] was approximately 3 times higher than in the Sea of Okhotsk [the mean of (0.22 ± 0.16) kg·m^{-3}] (see Table 1).

In the Pacific Ocean, density stratification occurred within the Z_{eu} throughout the entire area we studied. Nevertheless, in the Sea of Okhotsk, density stratification at some stations occurred deeper than the Z_{eu} (Table 1). Due to density stratification within the Z_{eu}, two water layers differing in conditions were formed: the UML and the layer below the UML. The Z_{UML} varied significantly (from 2 to 24 m) for the entire study area. The Sea of Okhotsk featured deeper UML [the mean of (11.0 ± 6.3) m] than the Pacific Ocean [the mean of (3.9 ± 2.4) m].

Vertical distribution of chlorophyll *a* fluorescence was characterized by homogeneous fluorescence intensity within the UML. At some stations, deep maximum of chlorophyll *a* fluorescence was observed in the thermocline or below (Fig. 2).

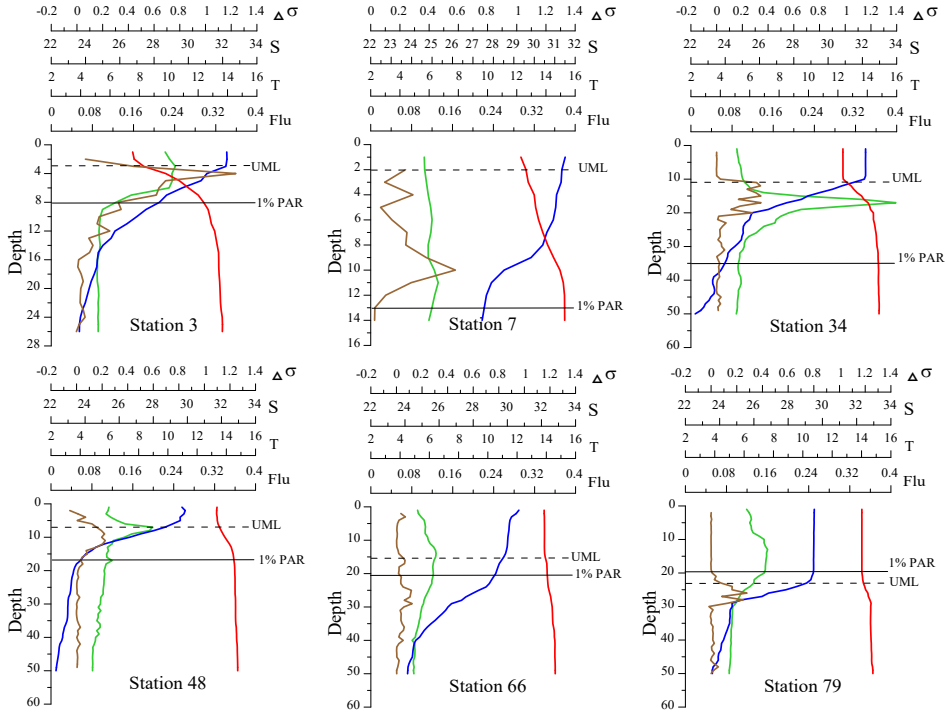

Fig. 2. Examples of vertical profiles of chlorophyll *a* fluorescence (Flu, the green line), temperature (T, °C, the blue line), salinity (S, psu, the red line), and density gradient (Δσ, kg·m^{-3}, the brown line) in waters near the Kamchatka Peninsula in August–September 2023. The black solid line is the euphotic zone, and the black dotted line is the upper mixed layer

Рис. 2. Примеры вертикальных профилей флуоресценции хлорофилла *a* (Flu, зелёная линия), температуры (T, °C, синяя линия), солёности (S, PSU, красная линия) и градиента плотности (Δσ, кг·м$^{-3}$, коричневая линия) в шельфовых водах полуострова Камчатка в августе — сентябре 2023 г. Чёрная сплошная линия — глубина зоны фотосинтеза; чёрная пунктирная линия — глубина верхнего квазиоднородного слоя

Rapid light–response curves of variable fluorescence. Phytoplankton photoacclimation at stations with different hydrological properties (in the Z_{eu} in particular) resulted in distinct patterns of rETR *vs.* PFD curves (Fig. 3). As shown, rETR values rose with PFD until reaching a "plateau" of light-saturated values. Typically, initial phase of RLCs featured a more rapid increase in rETR. Phytoplankton was acclimated to higher light intensities in the surface layer and in UML; therefore, RLCs of rETR reached saturation at higher PFD than in the layer below the UML. In some cases, rETR gradually decreased after the maximum ($rETR_{max}$, a "plateau"), which reflected photoinhibition induced by high irradiance.

In the surface layer, $rETR_{max}$ was a highly variable parameter (values varied from 48 to 160) (Table 2, Fig. 4). Moreover, it decreased gradually with depth, down to a minimum of (51 ± 16) near the bottom of the Z_{eu} due to a drop in PAR. Phytoplankton in the UML was characterized by higher $rETR_{max}$ values [the mean of (72 ± 14)] compared to phytoplankton in the layer below the UML [the mean of (53 ± 19)] ($p < 0.0001$). RLCs of rETR in the UML were saturated under higher irradiance [the mean of (240 ± 44) μmol·m^{-2}·s^{-1}] than in the layer below the UML [the mean of (170 ± 55) μmol·m^{-2}·s^{-1}] ($p < 0.0001$). I_k in the surface layer, the same as $rETR_{max}$, varied noticeably: by about three times, 160 to 480 μmol·m^{-2}·s^{-1} (Table 2, Fig. 4). The values of I_k decreased gradually with depth, down to ~ 80 μmol·m^{-2}·s^{-1} near the bottom of the Z_{eu}. Values of α also varied significantly in the surface layer: by about 1.5 times, 0.21 to 0.35 μmol^{-1}·m^{-2}·s^{-1} (Table 2, Fig. 4). The values of α in the UML and in the layer below the UML fluctuated in a similar range, 0.025 to 0.40 μmol·m^{-2}·s^{-1}, and had similar mean value, (0.31 ± 0.024) μmol·m^{-2}·s^{-1} ($p = 0.05$).

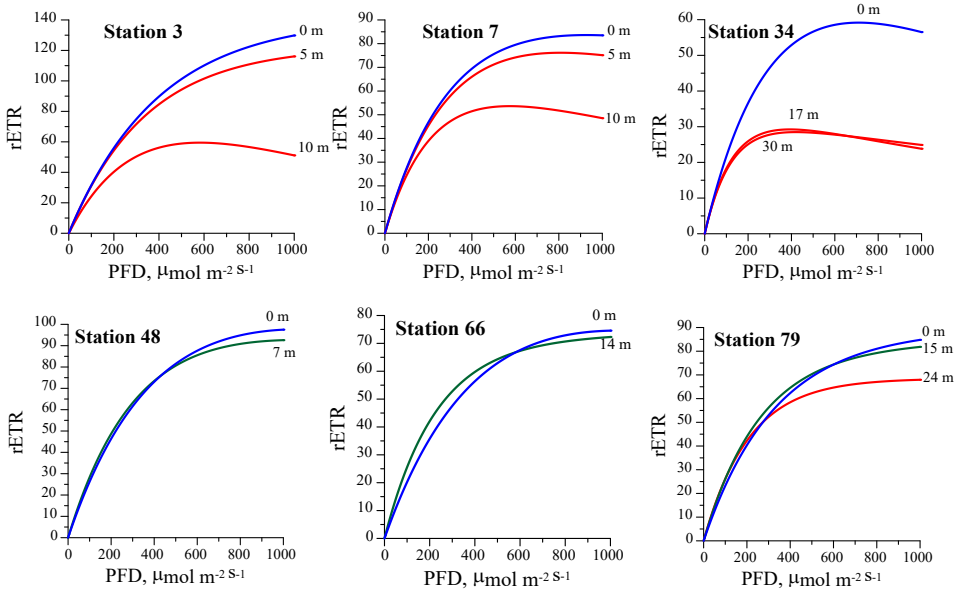

Fig. 3. Rapid light–response curves (RLCs) of relative electron transport rate (rETR) in phytoplankton at various depths of euphotic zone in waters near the Kamchatka Peninsula in August–September 2023: at the surface (the blue line), in the upper mixed layer (the green line), and in the layer below the upper mixed layer (the red line)

Рис. 3. Быстрые световые кривые (RLC) относительной скорости транспорта электронов (rETR) фитопланктона с разных глубин зоны фотосинтеза в шельфовых водах полуострова Камчатка в августе и сентябре 2023 г. — в поверхностном слое (синяя линия), в верхнем квазиоднородном слое (зелёная линия) и в слое под верхним квазиоднородным слоем (красная линия)

Table 2. Phytoplankton photosynthetic parameters in waters near the Kamchatka Peninsula in August–September 2023: maximum relative electron transport rate ($rETR_{max}$), light-saturation coefficient (I_k), tangent of initial slope of the rapid light–response curve of rETR (α), and maximum quantum yield of primary photochemistry of photosystem II (F_v/F_m)

Таблица 2. Фотосинтетические характеристики фитопланктона в шельфовых водах полуострова Камчатка в августе — сентябре 2023 г.: максимальная относительная скорость транспорта электронов ($rETR_{max}$), коэффициент насыщения светом (I_k), тангенс начального наклона быстрой световой кривой rETR (α) и максимальный квантовый выход фотохимических реакций в фотосистеме II (F_v/F_m)

	$rETR_{max}$	I_k, µmol·m^{-2}·s^{-1}	α, µmol^{-1}·m^{-2}·s^{-1}	F_v/F_m
Sea surface				
Mean	84	290	0.29	0.57
SD	18	51	0.032	0.092
Min	48	160	0.21	0.31
Max	160	480	0.35	0.70
Upper mixed layer				
Mean	72	240	0.30	0.64
SD	14	44	0.019	0.055
Min	36	120	0.25	0.51
Max	100	340	0.34	0.71
Layer below the upper mixed layer				
Mean	53	170	0.31	0.66
SD	19	55	0.024	0.038
Min	25	84	0.25	0.56
Max	120	340	0.40	0.77

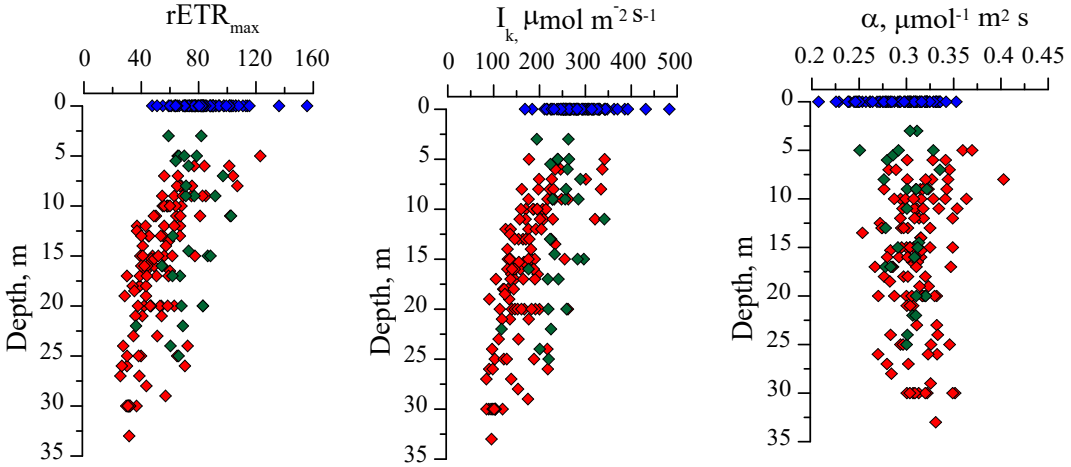

Fig. 4. Vertical distribution of the maximum relative electron transport rate ($rETR_{max}$), the light-saturation coefficient (I_k), and the tangent of initial slope of the rapid light–response curve of rETR (α) in waters near the Kamchatka Peninsula in August–September 2023: at the surface (♦), in the upper mixed layer (♦), and in the layer below the upper mixed layer (♦)

Рис. 4. Вертикальное распределение значений максимальной относительной скорости транспорта электронов ($rETR_{max}$), коэффициента насыщения светом (I_k) и тангенса начального наклона быстрой световой кривой rETR (α) в водах у полуострова Камчатка в августе — сентябре 2023 г.: в поверхностном слое (♦), в верхнем квазиоднородном слое (♦) и в слое под верхним квазиоднородным слоем (♦)

Maximum quantum yield of photosystem II. For the data obtained in the Pacific Ocean and the Sea of Okhotsk, noticeably different values of F_v/F_m (0.31–0.70) were recorded in the surface layer (Fig. 5). In the UML and the layer below the UML, the range of F_v/F_m values was narrower by 1.5 times (0.51–0.77) than that registered for the surface layer. The UML and the layer below the UML did not differ statistically significantly in terms of F_v/F_m ($p = 0.43$). The values of F_v/F_m near the bottom of the Z_{eu} averaged (0.67 ± 0.04).

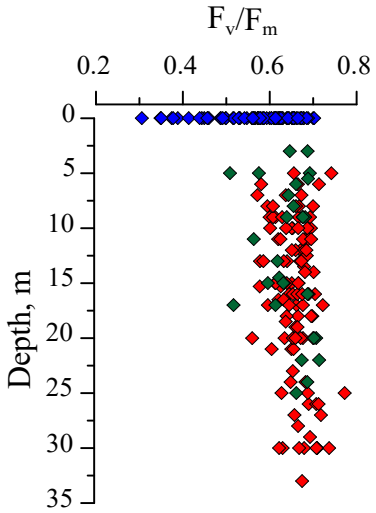

Fig. 5. Vertical distribution of the maximum quantum yield of primary photochemistry of photosystem II (F_v/F_m) in waters near the Kamchatka Peninsula in August–September 2023: at the surface (♦), in the upper mixed layer (♦), and in the layer below the upper mixed layer (♦)

Рис. 5. Вертикальное распределение значений максимального квантового выхода фотохимических реакций в фотосистеме II (F_v/F_m) в водах у полуострова Камчатка в августе — сентябре 2023 г.: в поверхностном слое (♦), в верхнем квазиоднородном слое (♦) и в слое под верхним квазиоднородным слоем (♦)

The relationship was established between F_v/F_m values in the surface water layer and the sampling time (Fig. 6). During daylight hours, F_v/F_m in phytoplankton sampled before midday reached their maximums: F_v/F_m values varied from 0.49 to 0.70. In phytoplankton sampled in the afternoon, F_v/F_m values were lower ($p < 0.0001$) and varied from 0.31 to 0.66.

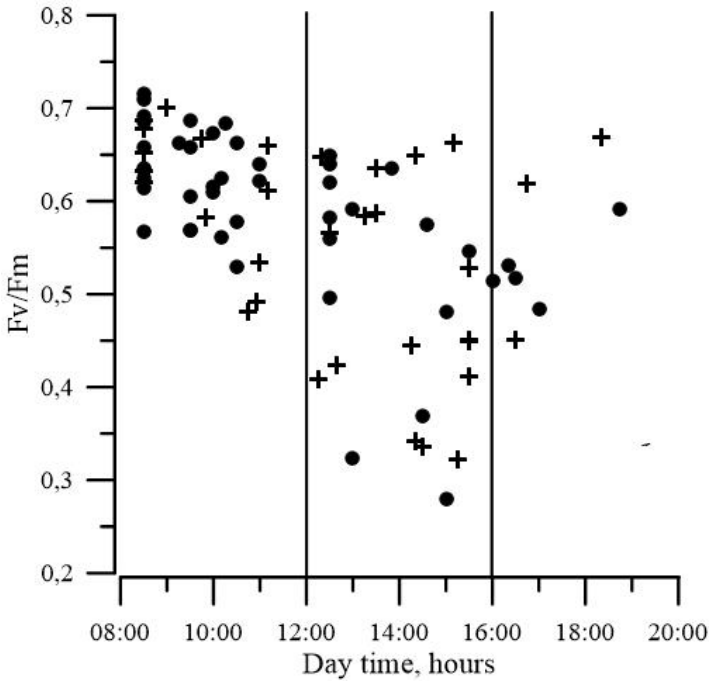

Fig. 6. Dependence of the maximum quantum yield of primary photochemistry of photosystem II (F_v/F_m) in the surface water layer on the sampling time near the Kamchatka Peninsula in August–September 2023: in the Pacific Ocean (●) and the Sea of Okhotsk (+). The black solid lines divide the time axis into four-hour intervals

Рис. 6. Зависимость максимального квантового выхода фотохимических реакций в фотосистеме II (F_v/F_m) в поверхностном слое вод у полуострова Камчатка в августе — сентябре 2023 г. от времени отбора проб в Тихом океане (●) и Охотском море (+). Чёрные сплошные линии разделяют ось времени на четырёхчасовые интервалы

F_v/F_m in the surface water layer varied due to the inhibitory effect of high PAR_0 values at the sampling time, and this was especially evident during midday and in the afternoon. Fig. 7 shows the dynamics of F_v/F_m and PAR_0 during daylight hours, and also the values of daily PAR_0 on the sampling day. The daily PAR_0 varied by an order of magnitude: from 4.7 to 38 mol·m^{-2}·day^{-1}. During sampling, PAR_0 attained ~ 1,600 μmol·m^{-2}·s^{-1} at some stations. Analysis of the daily dynamics of F_v/F_m showed the match of F_v/F_m minimum with PAR_0 maximum incident on the sea surface at the sampling time. Thus, the short-term response of F_v/F_m to change in ambient irradiance was shown.

The entire F_v/F_m data array for the surface layer was divided into three groups based on PAR_0 at the sampling time:

- group 1, $PAR_0 < 500$ μmol·m^{-2}·s^{-1};
- group 2, 500 μmol·m^{-2}·s^{-1} < PAR_0 < 1,000 μmol·m^{-2}·s^{-1};
- group 3, $PAR_0 > 1{,}000$ μmol·m^{-2}·s^{-1}.

The values of F_v/F_m in these three groups varied statistically significantly ($p < 0.0001$). The lowest F_v/F_m values, the mean of (0.50 ± 0.09), were obtained in group 3, while the highest, the mean of (0.63 ± 0.05), were recorded in group 1. The values of F_v/F_m in group 2 averaged (0.54 ± 0.09).

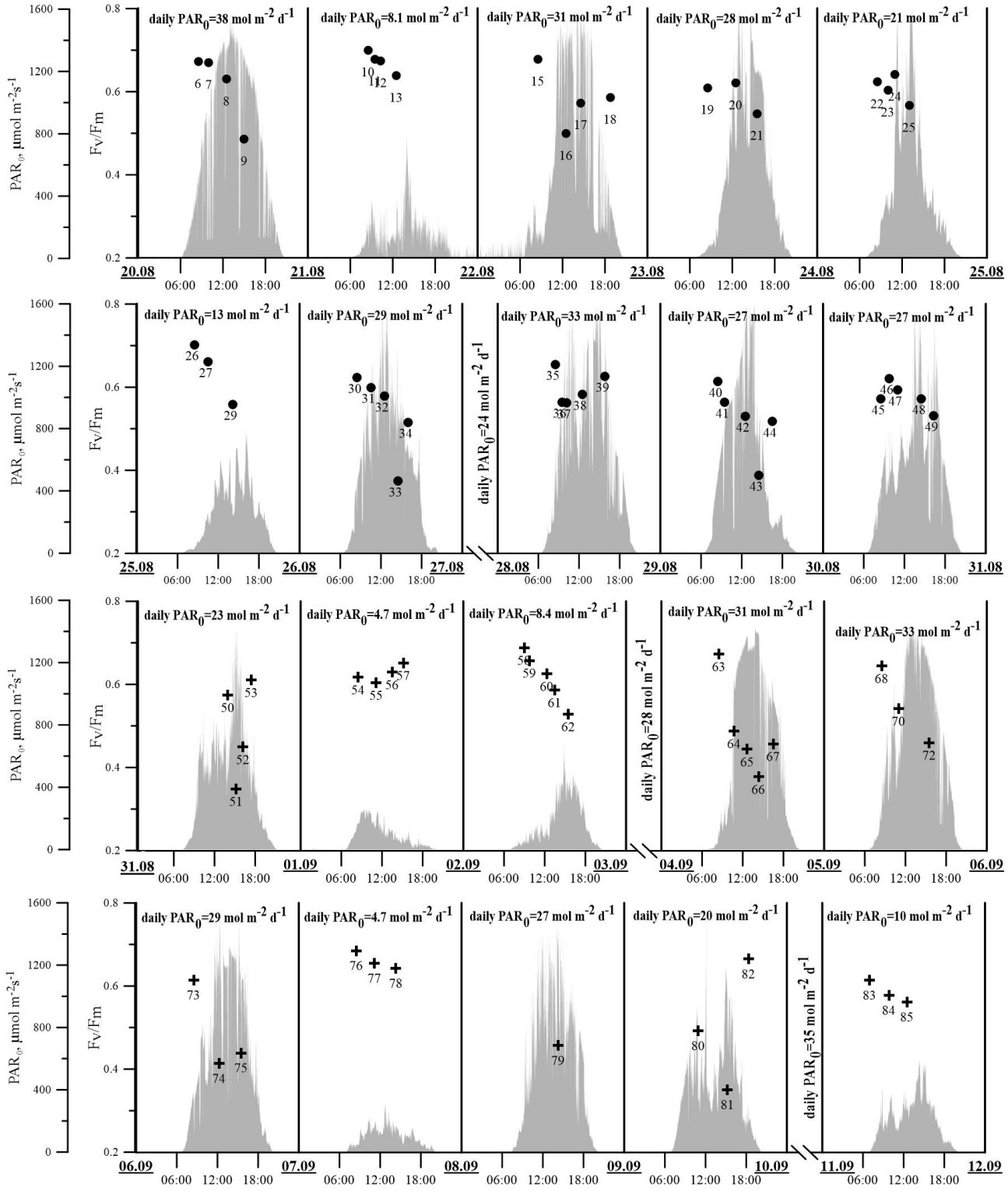

Fig. 7. Daily dynamics of the maximum quantum yield of primary photochemistry of photosystem II (F_v/F_m) and photosynthetically available radiation incident on the surface layer (PAR_0) at the sampling time in waters near the Kamchatka Peninsula in August–September 2023: in the Pacific Ocean (●) and the Sea of Okhotsk (+). The numbers indicate the stations

Рис. 7. Суточная динамика значений максимального квантового выхода фотохимических реакций фотосистемы II (F_v/F_m) и фотосинтетически активной радиации, падающей на поверхностность моря в момент отбора проб (PAR_0), в шельфовых водах полуострова Камчатка в августе и сентябре 2023 г. — в Тихом океане (●) и Охотском море (+). Цифрами обозначены номера станций

Maximum quantum yield of photosynthesis. For the entire data array (the Pacific Ocean and the Sea of Okhotsk), ϕ_{max} varied by six times: from 0.0091 to 0.057 mol C / mol quanta. In the surface layer, the values of ϕ_{max} fluctuated in a similar range: from 0.0091 to 0.047 mol C / mol quanta. Near the bottom of the Z_{eu}, a range of ϕ_{max} variations was narrow, from 0.044 to 0.058 mol C / mol quanta, and the mean was (0.047 ± 0.006) mol C / mol quanta (Fig. 8). Highly significant ($p < 0.0001$) inverse relationship was revealed between ϕ_{max} and daily PAR, and it was described by an exponential function (Fig. 8).

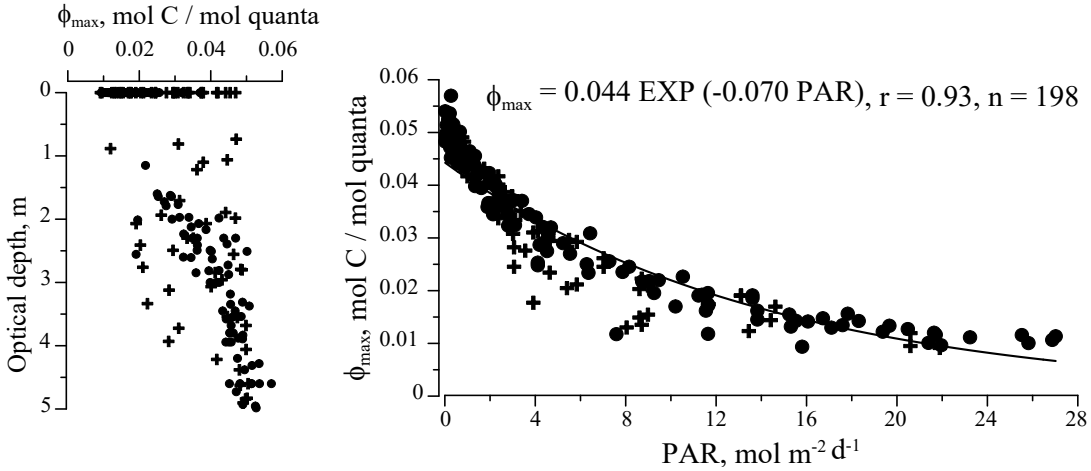

Fig. 8. Dependence of the maximum quantum yield of photosynthesis (ϕ_{max}) on the photosynthetically available radiation at sampling depths (PAR) in waters near the Kamchatka Peninsula in August–September 2023: in the Pacific Ocean (●) and the Sea of Okhotsk (+)

Рис. 8. Зависимость максимального квантового выхода фотосинтеза (ϕ_{max}) от величины фотосинтетически активной радиации на глубине отбора проб (PAR) в шельфовых водах полуострова Камчатка в августе и сентябре 2023 г. — в Тихом океане (●) и Охотском море (+)

DISCUSSION

Phytoplankton photosynthetic characteristics in the euphotic layer of waters near the Kamchatka Peninsula were analyzed based on parameters of variable chlorophyll *a* fluorescence. In the Pacific Ocean, sampling covered a period of relatively good weather (sea was calm). Under such conditions, the hydrological structure of the Pacific Ocean waters featured vertical density stratification within the Z_{eu} with the relatively narrow UML (maximum of 13 m at st. 41). In coastal waters of the Sea of Okhotsk, sampling was carried out when meteorological conditions deteriorated. Namely, wind speed increased; this resulted in active mixing of surface waters and in the UML deepening to the bottom of the Z_{eu} at some stations. Thus, Z_{UML}/Z_{eu} varied in this area from 0.1 to 1.3. In a relatively narrower UML, phytoplankton deals with higher PAR_{UML} than in the case when the UML is comparable with the Z_{eu}. Phytoplankton photosynthetic parameters shifted due to its adaptation to different environmental factors in the UML. Variable chlorophyll *a* fluorescence is a reliable indicator of photosynthetic parameters of phytoplankton. Effect of environmental factors on photosynthetic characteristics can be described by RLCs [Schreiber, 2004; Serôdio et al., 2006], since RLCs of variable fluorescence are dependent on phytoplankton "light history" [Cruz, Serôdio, 2008; Perkins et al., 2006]. The outcomes of this study showed that the shape of RLC of rETR depended on the phytoplankton photoacclimation to different light conditions within the layer. Although the shape of rETR photoresponse was mostly the same for phytoplankton inhabiting different layers, the absolute values of $rETR_{max}$ and I_k differed, as well as their variability range. In more insolated layers (the surface and the UML), phytoplankton featured higher values of $rETR_{max}$ and I_k than phytoplankton inhabiting a lower and less

insolated Z_{eu} (the layer below the UML) (see Fig. 6). For the entire data array (covering the surface layer, the UML, and the layer below the UML), the relationship of I_k and $rETR_{max}$ with daily PAR was revealed ($p < 0.0001$) (Fig. 9).

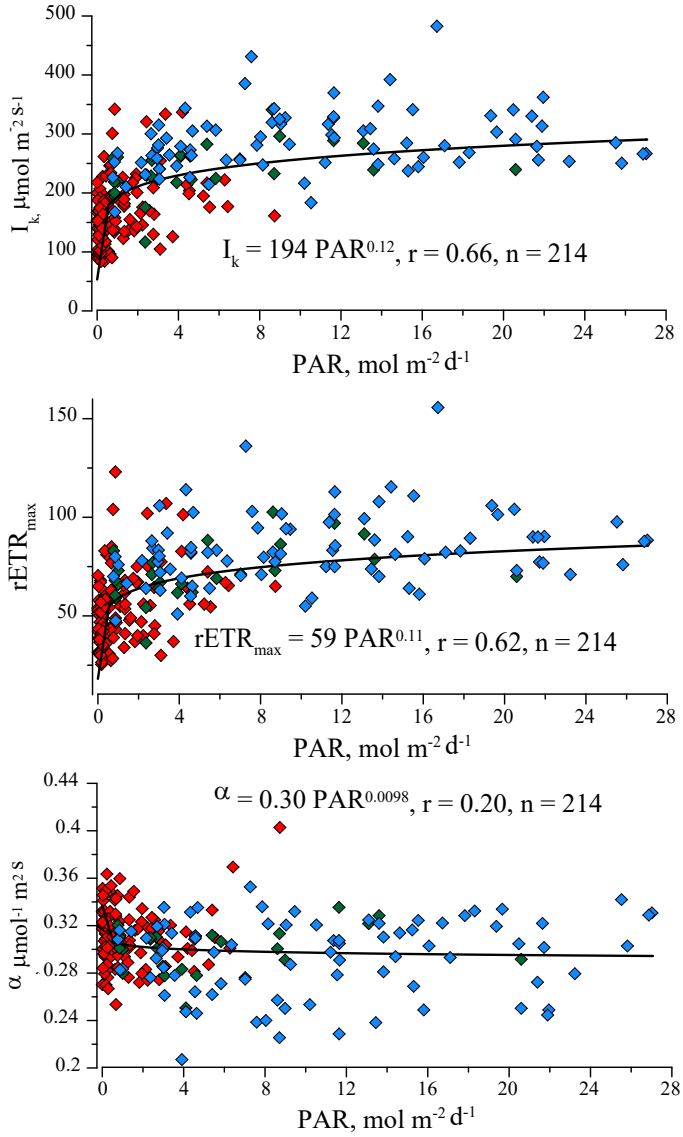

Fig. 9. Dependence of the light-saturation coefficient (I_k), the maximum relative electron transport rate ($rETR_{max}$), and the tangent of initial slope of the rapid light–response curve (α) on the daily photosynthetically available radiation in the environment (PAR): at the surface (♦), in the upper mixed layer (♦), and in the layer below the upper mixed layer (♦)

Рис. 9. Зависимость значений коэффициента насыщения светом (I_k), максимальной относительной скорости транспорта электронов ($rETR_{max}$) и тангенса начального наклона быстрой световой кривой (α) от суточной фотосинтетически активной радиации в среде (PAR): в поверхностном слое (♦), в верхнем квазиоднородном слое (♦) и в слое под верхним квазиоднородным слоем (♦)

The values of I_k and $rETR_{max}$ were characterized by a steep increase under low PAR and a smooth increase under PAR exceeding 1 mol·m^{-2}·day^{-1}. However, no relationship was revealed between α and PAR ($p = 0.003$) (see Fig. 9). Light-dependent variability of $rETR_{max}$ and I_k was in agreement with variability of these photosynthetic parameters due to phytoplankton photoacclimation [Behrenfeld et al., 2004; MacIntyre et al., 2002]. The photoacclimation is accompanied by changes in concentration and activity of enzymes of the Calvin cycle and in changes in the photosynthetic electron transport

chain, resulting in the $rETR_{max}$ variability [Behrenfeld et al., 2004; MacIntyre et al., 2002]. Notably, in the present study, no significant photoadaptive changes in α were noted (see Figs 6, 9). However, shifts in α could be expected, since changes in the content of photosynthetic accessory pigment or other components of the photosynthetic apparatus affecting the photoprotection capacity were recorded in other studies, *e. g.*, in [Woźniak et al., 2007].

Photoinhibition of the maximum quantum yield of primary photochemistry of PSII (F_v/F_m) was observed in the surface layer of the study area (the Pacific Ocean and the Sea of Okhotsk). The obtained wide range of F_v/F_m variability in the surface layer (Fig. 5) is due to differences in PAR_0 and the sampling time, since they determine "light history" (Figs 6, 7). The variability in F_v/F_m is mediated by changes in physiological state of photoautotrophs due to environmental factors [Schreiber, 2004]. The maximum achievable F_v/F_m value is 0.80–0.85 [Björkman, Demmig, 1978]. F_v/F_m depends on environmental factors: light [Heraud, Beardall, 2000; Vassiliev et al., 1994], nutrient availability [Beardall et al., 2001; Behrenfeld, Kolber, 1999; Lindley et al., 1995], and temperature [Wu et al., 2012], as well as on phytoplankton species composition [Suggett et al., 2009]. However, light is the key driver of F_v/F_m changes. Exposure to high light intensities results in photoinhibition: photosynthesis rate decreases in response to prolonged excess absorption of light quanta [Baker, 1996]. Phytoplankton of the upper water layer is most susceptible to photoinhibition, since it lives under relatively high light intensity. The analysis of F_v/F_m variability showed inverse relationship between F_v/F_m and PAR_0 at the sampling time ($p < 0.0001$) (Fig. 10). Minimum values of F_v/F_m (< 0.50) were obtained at relatively high PAR (> 750 $\mu E \cdot m^{-2} \cdot s^{-1}$), indicating an inhibitory effect of high light intensity. Photoinhibition of phytoplankton was governed by destruction of D1 protein of PSII reaction center [Chow, Aro, 2005]. The restoration of F_v/F_m during the night and the fact that it reaches its maximum in the early morning (Figs 6, 7) are related to D1 protein restoration in the dark [Chow, Aro, 2005]. In the UML and the layer below the UML, where PAR was lower than at the surface, changes in F_v/F_m values were weakly expressed, and F_v/F_m values were close to the maximum achievable magnitude (see Fig. 5).

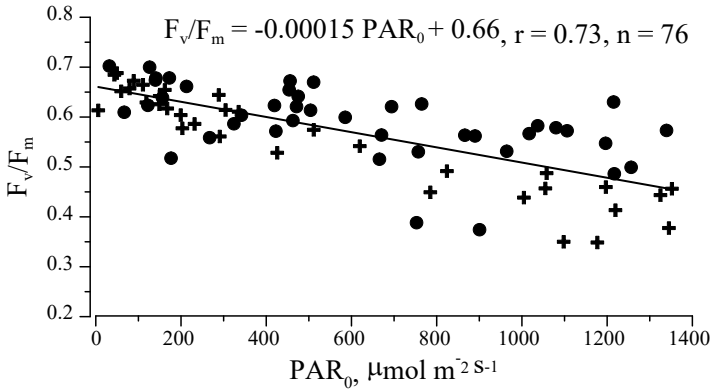

Fig. 10. Dependence of the maximum quantum yield of primary photochemistry of photosystem II (F_v/F_m) in the surface layer on the photosynthetically available radiation incident on the surface layer (PAR_0) at the sampling time in waters near the Kamchatka Peninsula in August–September 2023: in the Pacific Ocean (●) and the Sea of Okhotsk (+)

Рис. 10. Зависимость значений максимального квантового выхода фотохимических реакций фотосистемы II (F_v/F_m) в поверхностном слое моря от фотосинтетически активной радиации, падающей на поверхность моря в момент отбора проб (PAR_0), в шельфовых водах полуострова Камчатка в августе и сентябре 2023 г. — в Тихом океане (●) и Охотском море (+)

The values of ϕ_{max} rose while PAR decreased (Fig. 8). The obtained range of ϕ_{max} was in good agreement with the data of earlier studies covering the Pacific Ocean [Bricaud et al., 2002; Lindley et al., 1995; Vijayan et al., 2009] and the Sea of Okhotsk [Isada et al., 2013], where ϕ_{max} values

in the surface layer were generally about 10–40% of the theoretical maximum, 0.125 mol C / mol quanta, and even reached 0.1 under some environmental factors. Research on ϕ_{max} variability in various regions of the World Ocean showed as follows: the values of ϕ_{max} in eutrophic waters (~ 0.05 mol C / mol quanta) were higher than in mesotrophic waters (~ 0.035 mol C / mol quanta) and oligotrophic waters (~ 0.005 mol C / mol quanta) [Babin et al., 1996]. It was also shown that ϕ_{max} values depend on nutrient availability [Johnson et al., 2002; Kolber et al., 1990] and/or on taxonomic composition of phytoplankton populations [Babin et al., 1996; Cota et al., 1994]. Cyclic electron flow around photosystem I (PSI) can reduce ϕ_{max}. The cycle is related to the ratio of PSII-to-PSI reaction centers, which is > 1 in diatoms, ~ 1 in prochlorophytes, and ~ 0.25 in cyanobacteria [Babin et al., 1996]. However, the irradiance has the maximum effect on ϕ_{max} values [Babin et al., 1996; Woźniak et al., 2007].

The values of ϕ varied by an order of magnitude: from 0.0046 to 0.057 mol C / mol quanta. Importantly, ϕ, the same as ϕ_{max}, depends chiefly on light intensity [Woźniak et al., 2007]. However, light affects values of ϕ to a greater extent than values of ϕ_{max}, and this is especially evident at high light intensities (Figs 8, 11) due to non-photochemical dissipation of the absorbed excitation energy, mainly as heat [Kirk, 2011; Woźniak et al., 2007]. A tight relationship between values of ϕ and daily PAR ($p < 0.0001$) (PAR_{UML} for the UML and PAR_Z for the layer below the UML) was revealed; it was described by an exponential function (see Fig. 11).

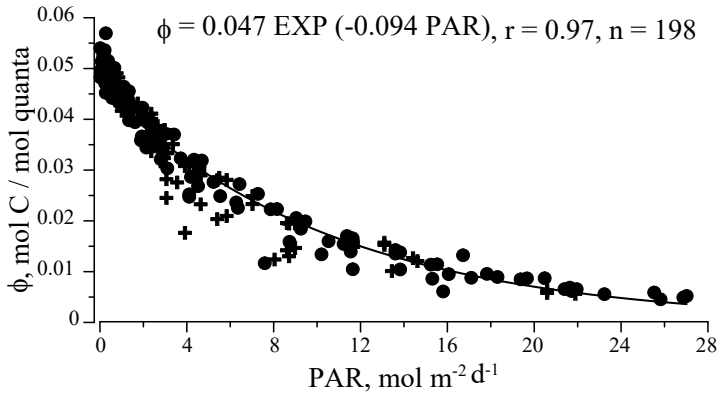

Fig. 11. Dependence of the quantum yield of photosynthesis (ϕ) on the daily photosynthetically available radiation in the environment (PAR) in waters near the Kamchatka Peninsula in August–September 2023: in the Pacific Ocean (●) and the Sea of Okhotsk (+)

Рис. 11. Зависимость значений квантового выхода фотосинтеза (ϕ) от суточной фотосинтетически активной радиации в среде (PAR) в шельфовых водах полуострова Камчатка в августе и сентябре 2023 г. — в Тихом океане (●) и Охотском море (+)

Conclusion. We studied the variability of the key photosynthetic parameters of phytoplankton: the quantum yield of photosynthesis, its maximum value, and also the light-saturating coefficient – in waters of the Pacific Ocean and the Sea of Okhotsk off the southern Kamchatka Peninsula coast in August–September 2023.

Reliable differences in the values of ϕ_{max} and I_k were revealed between the quasi-isolated layers within the euphotic zone: the upper mixed layer (UML) and the layer below UML.

High variability of the photosynthetic parameters was observed in each selected layer; it was caused by high heterogeneity of the study area in terms of the hydrological structure. Thus, the pycnocline was located within the euphotic zone (Z_{UML}/Z_{eu} varied from 0.1 to 1.3), which was the real physical boundary between the layers. As a result, each layer featured high spatial heterogeneity in environmental factors, mainly in light.

As shown, I_k values were directly related to light intensity. Nonetheless, the values of ϕ_{max} were inversely related to light intensity, but to a larger extent than I_k. Accordingly, ϕ, which depended on I_k and ϕ_{max}, dropped while light intensity increased. The relationships between the phytoplankton photosynthetic parameters (ϕ_{max}, ϕ, and I_k) and light intensity were revealed, which allows assessing phytoplankton photosynthetic parameters based on light in the case of highly variable hydrological structure of waters.

The application of chlorophyll a fluorescence measurements for the assessment of phytoplankton photosynthetic characteristics was carried out within the framework of IBSS state research assignment No. 124030100106-2. Analysis of light-dependent variability in photosynthetic characteristics of phytoplankton was funded by the Ministry of Science and Higher Education of the Russian Federation, project No. FZNS-2024-0037 "Integrated environmental monitoring of coastal marine and terrestrial ecosystems of Kamchatka." In situ measurements of chlorophyll a fluorescence were performed within the framework of POI FEB RAS state research assignment No. 124022100080-0.

Acknowledgement. We would like to thank the captain and crew of the RV "Professor Multanovskiy" for their help in the expeditionary work. We thank Dar'ya Davydova, Alena Sausheva, and Mikhail Samoilov for assistance in sampling. We owe our deep gratitude to Anatoly Buchelnikov for his help with software. We thank anonymous reviewers for detailed critical comments on the manuscript.

REFERENCES

1. Antal T., Konyukhov I., Volgusheva A., Plyusnina T., Khruschev S., Kukarskikh G., Rubin A. Chlorophyll fluorescence induction and relaxation system for the continuous monitoring of photosynthetic capacity in photobioreactors. *Physiologia Plantarum*, 2019, vol. 165, no. 3, pp. 476–486. https://doi.org/10.1111/ppl.12693
2. Babin M. Phytoplankton fluorescence: Theory, current literature and *in situ* measurement. In: *Real-time Coastal Observing Systems for Marine Ecosystem Dynamics and Harmful Algal Blooms: Theory, Instrumentation and Modelling* / M. Babin, C. S. Roesler, J. J. Cullen (Eds). Paris : UNESCO Publishing, 2008, pp. 237–280.
3. Babin M., Morel A., Claustre H., Bricaud A., Kolber Z., Falkowski P. G. Nitrogen- and irradiance-dependent variations of the maximum quantum yield of carbon fixation in eutrophic, mesotrophic and oligotrophic marine systems. *Deep Sea Research Part I: Oceanographic Research Papers*, 1996, vol. 43, iss. 8, pp. 1241–1272. https://doi.org/10.1016/0967-0637(96)00058-1
4. Baker N. R. Photoinhibition of photosynthesis. In: *Light as an Energy Source and Information Carrier in Plant Physiology* / R. C. Jennings, G. Zucchelli, F. Ghetti, G. Colombetti (Eds). Boston, MA : Springer US, 1996, pp. 89–97. https://doi.org/10.1007/978-1-4613-0409-8
5. Bannister T. T. Quantitative description of steady state, nutrient-saturated algal growth, including adaptation. *Limnology and Oceanography*, 1979, vol. 24, iss. 1, pp. 76–96. https://doi.org/10.4319/lo.1979.24.1.0076
6. Beardall J., Young E., Roberts S. Approaches for determining phytoplankton nutrient limitation. *Aquatic Sciences*, 2001, vol. 63, iss. 1, pp. 44–69. https://doi.org/10.1007/pl00001344
7. Behrenfeld M. J., Kolber Z. S. Widespread iron limitation of phytoplankton in the south Pacific Ocean. *Science*, 1999, vol. 283, no. 5403, pp. 840–843. https://doi.org/10.1126/science.283.5403.840
8. Behrenfeld M. J., Prasil O., Babin M., Bruyant F. In search of a physiological basis for covariations in light-limited and light-saturated photosynthesis. *Journal of Phycology*, 2004, vol. 40, iss. 1, pp. 4–25. https://doi.org/10.1046/j.1529-8817.2004.03083.x
9. Björkman O., Demmig B. Photon yield of O_2 evolution and chlorophyll fluorescence characteristics at 77 K among vascular plants of diverse origins. *Planta*, 1987, vol. 170, iss. 4, pp. 489–504. https://doi.org/10.1007/bf00402983
10. Brainerd K. E., Gregg M. C. Surface mixed and mixing layer depths. *Deep Sea Research Part I: Oceanographic Research Papers*, 1995, vol. 42, iss. 9, pp. 1521–1543. https://doi.org/10.1016/0967-0637(95)00068-h
11. Bricaud A., Roesler C. S., Parslow J. S., Ishizaka J. Bio-optical studies during

the JGOFS-equatorial Pacific program: A contribution to the knowledge of the equatorial system. *Deep Sea Research Part II: Topical Studies in Oceanography*, 2002, vol. 49, iss. 13–14, pp. 2583–2599. https://doi.org/10.1016/s0967-0645(02)00049-8

12. Chow W. S, Aro E.-M. Photoinactivation and mechanisms of recovery. In: *Photosystem II. The Light-Driven Water: Plastoquinone Oxidoreductase* / T. Wydrzynski, K. Satoh (Eds). Netherlands : Springer, 2005, pp. 627–648. https://doi.org/10.1007/1-4020-4254-x
13. Churilova T., Suslin V., Krivenko O., Efimova T., Moiseeva N. Spectral approach to assessment of phytoplankton photosynthesis rate in the Black Sea based on satellite information methodological aspects of the regional model development. *Journal of Siberian Federal University. Biology*, 2016, vol. 9, iss. 4, pp. 367–384. (in Russ.). https://doi.org/10.17516/1997-1389-2016-9-4-367-384
14. Cota G. F., Smith W. O., Mitchell B. G. Photosynthesis of *Phaeocystis* in the Greenland Sea. *Limnology and Oceanography*, 1994, vol. 39, iss. 4, pp. 948–553. https://doi.org/10.4319/lo.1994.39.4.0948
15. Cruz S., Serôdio J. Relationship of rapid light curves of variable fluorescence to photoacclimation and non-photochemical quenching in a benthic diatom. *Aquatic Botany*, 2008, vol. 88, iss. 3, pp. 256–264. https://doi.org/10.1016/j.aquabot.2007.11.001
16. *Evolution of Primary Producers in the Sea* / P. Falkowski, A. H. Knoll (Eds). New York ; London ; Oxford : Academic Press, 2011, 441 p. https://doi.org/10.1016/b978-0-12-370518-1.x5000-0
17. Falkowski P. G., Raven J. A. *Aquatic Photosynthesis.* 2nd edition. New Jersey : Princeton University Press, 2007, 488 p.
18. Heraud P., Beardall J. Changes in chlorophyll fluorescence during exposure of *Dunaliella tertiolecta* to UV radiation indicate a dynamic interaction between damage and repair processes. *Photosynthesis Research*, 2000, vol. 63, iss. 2, pp. 123–134. https://doi.org/10.1023/a:1006319802047
19. IOCCG. *Ocean Optics and Biogeochemistry Protocols for Satellite Ocean Colour Sensor Validation, Volume 4.0. Inherent Optical Property Measurements and Protocols: Best Practices for the Collection and Processing of Ship-Based Underway Flow-Through Optical Data* / A. R. Neeley, A. Mannino (Eds). Dartmouth, NS, Canada : International Ocean-Colour Coordinating Group (IOCCG), 2019, 22 p. (IOCCG Protocol Series ; vol. 4.0). https://doi.org/10.25607/obp-664
20. Isada T., Iida T., Liu H., Saitoh S. I., Nishioka J., Nakatsuka T., Suzuki K. Influence of Amur River discharge on phytoplankton photophysiology in the Sea of Okhotsk during late summer. *Journal of Geophysical Research: Oceans*, 2013, vol. 118, iss. 4, pp. 1995–2013. https://doi.org/10.1002/jgrc.20159
21. Johnson Z., Bidigare R. R., Goericke R., Marra J., Trees C., Barber R. T. Photosynthetic physiology and physicochemical forcing in the Arabian Sea, 1995. *Deep Sea Research Part I: Oceanographic Research Papers*, 2002, vol. 49, iss. 3, pp. 415–436. https://doi.org/10.1016/s0967-0637(01)00068-1
22. Kirk J. T. O. *Light and Photosynthesis in Aquatic Ecosystems.* 3rd edition. Cambridge : Cambridge University Press, 2011, 662 p. https://doi.org/10.1017/cbo9781139168212
23. Kolber Z., Wyman K. D., Falkowski P. G. Natural variability in photosynthetic energy conversion efficiency: A field study in the Gulf of Maine. *Limnology and Oceanography*, 1990, vol. 35, iss. 1, pp. 72–79. https://doi.org/10.4319/lo.1990.35.1.0072
24. Lawrenz E., Silsbe G., Capuzzo E., Ylöstalo P., Forster R. M., Simis S. G., Suggett D. J. Predicting the electron requirement for carbon fixation in seas and oceans. *PloS One*, 2013, vol. 8, iss. 3, art. e58137 (18 p.). https://doi.org/10.1371/journal.pone.0058137
25. Laws E. A. Photosynthetic quotients, new production and net community production in the open ocean. *Deep Sea Research Part A. Oceanographic Research Papers*, 1991, vol. 38, iss. 1, pp. 143–167. https://doi.org/10.1016/0198-0149(91)90059-o
26. Lee Z., Weidemann A., Kindle J., Arnone R., Carder K. L., Davis C. Euphotic zone depth: Its derivation and implication to ocean-color remote sensing. *Journal of Geophysical Research: Oceans*, 2007, vol. 112, no. C3, art. C03009 (11 p.). https://doi.org/10.1029/2006jc003802
27. Lindley S. T., Bidigare R. R., Barber R. T. Phytoplankton photosynthesis parameters along 140°W in the equatorial Pacific. *Deep Sea Research*

Part II: Topical Studies in Oceanography, 1995, vol. 42, iss. 2–3, pp. 441–463. https://doi.org/10.1016/0967-0645(95)00029-p

28. MacIntyre H. L., Kana T. M., Anning T., Geider R. J. Photoacclimation of photosynthesis irradiance response curves and photosynthetic pigments in microalgae and cyanobacteria. *Journal of Phycology*, 2002, vol. 38, iss. 1, pp. 17–38. https://doi.org/10.1046/j.1529-8817.2002.00094.x
29. Marra J., Trees C. C., Bidigare R. R., Barber R. T. Pigment absorption and quantum yields in the Arabian Sea. *Deep Sea Research Part II: Topical Studies in Oceanography*, 2000, vol. 47, iss. 7–8, pp. 1279–1299. https://doi.org/10.1016/s0967-0645(99)00144-7
30. Morel A., Antoine D., Babin M., Dandonneau Y. Measured and modeled primary production in the northeast Atlantic (EUMELI JGOFS program): The impact of natural variations in photosynthetic parameters on model predictive skill. *Deep Sea Research Part I: Oceanographic Research Papers*, 1996, vol. 43, iss. 8, pp. 1273–1304. https://doi.org/10.1016/0967-0637(96)00059-3
31. Perkins R. G., Mouget J.-L., Lefebvre S., Lavaud J. Light response curve methodology and possible implications in the application of chlorophyll fluorescence to benthic diatoms. *Marine Biology*, 2006, vol. 149, iss. 4, pp. 703–712. https://doi.org/10.1007/s00227-005-0222-z
32. Platt T., Gallegos C. L., Harrison W. G. Photoinhibition of photosynthesis in natural assemblages of marine phytoplankton. *Journal of Marine Research*, 1980, vol. 38, pp. 687–701.
33. Platt T., Jassby A. D. The relationship between photosynthesis and light for natural assemblages of coastal marine phytoplankton. *Journal of Phycology*, 1976, vol. 12, iss. 4, pp. 421–430. https://doi.org/10.1111/j.1529-8817.1976.tb02866.x
34. Schreiber U. Pulse-amplitude-modulation (PAM) fluorometry and saturation pulse method: An overview. In: *Chlorophyll a Fluorescence. A Signature of Photosynthesis* / G. C. Papageorgiou, Govindjee (Eds). Dordrecht, the Netherlands : Springer, 2004, pp. 279–319. https://doi.org/10.1007/978-1-4020-3218-9
35. Schreiber U., Bilger W., Neubauer C. Chlorophyll fluorescence as a nonintrusive indicator for rapid assessment of *in vivo* photosynthesis. In: *Ecophysiology of Photosynthesis* / E.-D. Schulze, M. M. Caldwell (Eds). Berlin : Springer, 1994, pp. 49–70. https://doi.org/10.1007/978-3-642-79354-7
36. Schreiber U., Gademann R., Ralph P. J., Larkum A. W. D. Assessment of photosynthetic performance of *Prochloron* in *Lissoclinum patella* in hospite by chlorophyll fluorescence measurements. *Plant and Cell Physiology*, 1997, vol. 38, iss. 8, pp. 945–951. https://doi.org/10.1093/oxfordjournals.pcp.a029256
37. Serôdio J., Vieira S., Cruz S., Coelho H. Rapid light-response curves of chlorophyll fluorescence in microalgae: Relationship to steady-state light curves and non-photochemical quenching in benthic diatom-dominated assemblages. *Photosynthesis Research*, 2006, vol. 90, iss. 1, pp. 29–43. https://doi.org/10.1007/s11120-006-9105-5
38. Smyth T. J., Tilstone G. H., Groom S. B. Integration of radiative transfer into satellite models of ocean primary production. *Journal of Geophysical Research: Oceans*, 2005, vol. 110, iss. C10, pp. C10014.1–C10014.11. https://doi.org/10.1029/2004jc002784
39. Suggett D. J., Moore C. M., Hickman A. E., Geider R. J. Interpretation of fast repetition rate (FRR) fluorescence: Signatures of phytoplankton community structure *versus* physiological state. *Marine Ecology Progress Series*, 2009, vol. 376, pp. 1–19. https://doi.org/10.3354/meps07830
40. Vassiliev I. R., Prasil O., Wyman K. D., Kolber Z., Hanson Jr. A. K., Prentice J. E., Falkowski P. G. Inhibition of PS II photochemistry by PAR and UV radiation in natural phytoplankton communities. *Photosynthesis Research*, 1994, vol. 42, iss. 1, pp. 51–64. https://doi.org/10.1007/bf00019058
41. Vijayan A. K., Yoshikawa T., Watanabe S., Sasaki H., Matsumoto K., Saito S.-I., Takeda S., Furuya K. Influence of non-photosynthetic pigments on light absorption and quantum yield of photosynthesis in the western equatorial Pacific and the Subarctic North Pacific. *Journal of Oceanography*, 2009, vol. 65, iss. 2, pp. 245–258. https://doi.org/10.1007/s10872-009-0023-y
42. Woźniak B., Ficek D., Ostrowska M., Majchrowski R., Dera J. Quantum yield of photosynthesis in the Baltic: A new mathematical expression for remote sensing applications. *Oceanologia*, 2007, vol. 49, iss. 4, pp. 527–542.

43. Wu H., Roy S., Alami M., Green B. R., Campbell D. A. Photosystem II photoinactivation, repair, and protection in marine centric diatoms. *Plant Physiology*, 2012, vol. 160, iss. 1, pp. 464–476. https://doi.org/10.1104/pp.112.203067
44. Zhu Y., Ishizaka J., Tripathy S. C., Wang S., Mino Y., Matsuno T., Suggett D. J. Variation of the photosynthetic electron transfer rate and electron requirement for daily net carbon fixation in Ariake Bay, Japan. *Journal of Oceanography*, 2016, vol. 72, iss. 5, pp. 761–776. https://doi.org/10.1007/s10872-016-0370-4
45. Zhu Y., Ishizaka J., Tripathy S. C., Wang S., Sukigara C., Goes J., Matsuno T., Suggett D. J. Relationship between light, community composition and the electron requirement for carbon fixation in natural phytoplankton. *Marine Ecology Progress Series*, 2017, vol. 580, pp. 83–100. https://doi.org/10.3354/meps12310
46. Zhu Y., Suggett D. J., Liu C., He J., Lin L., Le F., Ishizaka J., Goes J., Hao Q. Primary productivity dynamics in the summer Arctic Ocean confirms broad regulation of the electron requirement for carbon fixation by light-phytoplankton community interaction. *Frontiers in Marine Science*, 2019, vol. 6, art. 275 (17 p.). https://doi.org/10.3389/fmars.2019.00275

ФОТОСИНТЕТИЧЕСКИЕ ХАРАКТЕРИСТИКИ ФИТОПЛАНКТОНА В ШЕЛЬФОВЫХ ВОДАХ ПОЛУОСТРОВА КАМЧАТКА В АВГУСТЕ — СЕНТЯБРЕ 2023 Г.

Т. В. Ефимова[1,2], Т. Я. Чурилова[1,2], Н. А. Моисеева[1], Е. Ю. Скороход[1,2], П. А. Салюк[3], А. В. Яцук[4]

[1]ФГБУН ФИЦ «Институт биологии южных морей имени А. О. Ковалевского РАН», Севастополь, Российская Федерация
[2]Лаборатория экологии и эволюционной биологии водных организмов, Институт Мирового океана, Дальневосточный федеральный университет, Владивосток, Российская Федерация
[3]Тихоокеанский океанологический институт имени В. И. Ильичёва ДВО РАН, Владивосток, Российская Федерация
[4]Научно-технологический университет «Сириус», Сириус, Российская Федерация
E-mail: *tatyana-iefimova@yandex.ru*

Изменение климата и возрастающая антропогенная нагрузка оказывают влияние на состояние водных экосистем. Продуктивность пелагических экосистем во многом определяется фотосинтетической способностью фитопланктона. Целью работы было проанализировать изменчивость фотосинтетических характеристик фитопланктона [квантового выхода фотосинтеза (ϕ), характеризующего эффективность использования поглощённых квантов света в процессе фотосинтеза, максимального квантового выхода (ϕ_{max}) и коэффициента насыщения светом (I_k)] в зависимости от световых условий, которые определяются отношением толщины верхнего квазиоднородного слоя (ВКС) к глубине зоны фотосинтеза. Использованы данные, полученных в шельфовых водах Тихого океана и Охотского моря в ходе рейса 23/4 НИС «Профессор Мультановский» в августе — сентябре 2023 г. Расчёт ϕ_{max} и I_k выполнен на основе измерения быстрых световых кривых флуоресценции. Установлено, что изменение фотосинтетических характеристик в основном обусловлено физиологической акклимацией фитопланктона к свету. В период сезонной стратификацией вод для ВКС и слоя зоны фотосинтеза, отличающихся по свету, получены существенно различающие по форме световые зависимости относительной скорости транспорта электронов. Показано, что величины I_k и ϕ_{max} разнонаправленно изменялись в зависимости от интенсивности света, при этом ϕ_{max} — в большей степени, чем I_k. В результате значение ϕ, зависящее от I_k и ϕ_{max}, уменьшалось с увеличением интенсивности света. Выявлена взаимосвязь между ϕ и интенсивностью света ($r = 0{,}97$; $p < 0{,}0001$), описанная экспоненциальной функцией. Обнаруженные зависимости I_k, ϕ_{max} и ϕ от интенсивности света могут быть использованы для экспресс-оценки их величин по данным интенсивности света в среде, что необходимо для анализа первичной продукции с применением спектрального подхода.

Ключевые слова: флуоресценция хлорофилла, фотоакклимация, быстрая световая кривая, квантовый выход фотосинтеза, Тихий океан, Охотское море